PRAMANA — journal of physics
© Indian Academy of Sciences
Vol. 82, No. 5
May 2014
pp. 823–830

Probing the density content of the nuclear symmetry energy

B K AGRAWAL*, J N DE and S K SAMADDAR
Saha Institute of Nuclear Physics, 1/AF Bidhan Nagar, Kolkata 700 064, India
*Corresponding author. E-mail: bijay.agrawal@saha.ac.in

DOI: 10.1007/s12043-014-0735-4; ***e*Publication:** 30 April 2014

Abstract. The nature of equation of state for the neutron star matter is crucially governed by the density dependence of the nuclear symmetry energy. We attempt to probe the behaviour of the nuclear symmetry energy around the saturation density by exploiting the empirical values for volume and surface symmetry energy coefficients extracted from the precise data on the nuclear masses.

Keywords. Symmetry energy; symmetry energy slope parameter; nuclear matter; neutron skin.

PACS Nos 21.65.Ef; 21.65.Mn; 21.10.Gv

1. Introduction

The study of symmetry energy is currently a subject of great interest. The nuclear symmetry energy and its density dependence play extremely important roles in the study of the structure of systems ranging from the atomic nucleus to the neutron star. The linear density dependence of the symmetry energy coefficient $C_{\rm v}(\rho)$ at density ρ is characterized by the slope parameter L defined as,

$$L = 3\rho \frac{{\rm d}C_{\rm v}(\rho)}{{\rm d}\rho}. \tag{1}$$

Particular attention is given to constrain, in a narrow window, the value of L at the nuclear matter saturation density $\rho_0 \sim 0.16\,{\rm fm}^{-3}$. The value of L at ρ_0 affects the nuclear binding energies and the nuclear drip lines and has a crucial role in determining the neutron density distribution in neutron-rich nuclei. The high-density behaviour of the equation of state for the neutron star matter is also governed by the values of L at supranormal densities ($\rho \gg \rho_0$). Such matter is highly asymmetric, is predominantly composed of neutrons and so the symmetry energy critically controls the nuclear pressure of such a system.

The symmetry energy is not a directly measurable quantity. It has to be extracted indirectly from various observables. One needs accurate knowledge of a large variety of

phenomena in order to map the nuclear symmetry energy over a wide range of density. The nuclear multifragmentation and cluster formation at low densities probe the nuclear symmetry energy at the subsaturation densities ($\rho < \rho_0$) [1,2]. The symmetry energy close to the nuclear saturation density can be probed by the neutron skin thickness and the isovector giant dipole resonances in heavy nucleus such as ^{208}Pb [3]. The high-density behaviour of the symmetry energy can be understood in terms of various observables associated with the neutron stars [4].

In this paper, we shall mainly focus on the behaviour of symmetry energy slope parameter L at densities close to ρ_0. The value of $L(\rho_0)$ has been shown [5] to be strongly correlated with the neutron skin thickness for ^{208}Pb nucleus. The neutron skin thickness denoted as $r_{\rm skin}$ is defined as the difference between the neutron and proton root mean square (rms) radii. The correlation of $L(\rho_0)$ with $r_{\rm skin}$ suggests that tight bounds on $L(\rho_0)$ requires knowledge of $r_{\rm skin}$ to be accurate within 0.5%. The information content of neutron skin thickness based on covariance analysis [6] once again points that $r_{\rm skin}$ is strongly correlated with $L(\rho_0)$. The lead radius experiment (PREX) [7,8] has recently measured $r_{\rm skin}$ of ^{208}Pb. This experiment is performed via parity-violating electron scattering [9] and provides the first purely electroweak, model-independent, measurement of the neutron distribution of a heavy nucleus. By measuring the neutron form factor of ^{208}Pb at momentum transfer $q \approx 0.475\,\text{fm}^{-1}$, PREX could determine $r_{\rm skin} = 0.33^{+0.16}_{-0.18}$ fm [8]. Alternatively, hadronic probes are used to estimate the neutron distribution in nuclei. However, these probes are model-dependent and display large theoretical uncertainties. The analyses from recent experiments have led to varying values of the neutron skin thickness, $r_{\rm skin} = 0.16 \pm 0.02(\text{stat.}) \pm 0.04(\text{syst.})$ fm and $r_{\rm skin} = 0.211^{+0.054}_{-0.063}$ fm. Nuclear dipole polarizability $\alpha_{\rm D}$ has been suggested [6,10] as an alternative observable constraining the neutron skin. The recent high resolution (p, p') measurement [11] of $\alpha_{\rm D}$ yields the neutron skin thickness of ^{208}Pb to be $0.156^{+0.025}_{-0.021}$ fm, but the model dependence [3] in the correlation between $r_{\rm skin}$ and $\alpha_{\rm D}$ assessed in systematic calculations in the framework of nuclear density functional theory is seen to shift the value of $r_{\rm skin}$ to $>0.168 \pm 0.022$ fm.

In the following sections, we present some of our recent results [12,13] for the values of $L(\rho_0)$ and $r_{\rm skin}$ of ^{208}Pb extracted using empirical values of the volume symmetry energy and surface symmetry energy coefficients [14] estimated from the available data on the nuclear masses. In §2, the theoretical formulation of the problem along with the results are presented. Section 3 contains the concluding remarks.

2. Density content of nuclear symmetry energy

The precise data on the nuclear masses for a large number of nuclei enables one to determine the values of the volume and surface symmetry energy coefficients within small uncertainties. In what follows, we use these informations to constrain the density content of the nuclear symmetry energy and the neutron skin thickness for ^{208}Pb nucleus. The symmetry energy coefficient, $a_{\rm sym}(A)$, for a nucleus with mass number A can be expressed in terms of $C_{\rm v}(\rho_0)$ and $C_{\rm s}$ as

$$a_{\rm sym}(A) = C_{\rm v}(\rho_0) - C_{\rm s} A^{-1/3}, \tag{2}$$

where $C_{\rm v}$ and $C_{\rm s}$ are the volume and surface symmetry energy coefficients, respectively. A meticulous study [14] of the double differences of 'experimental' symmetry energies

were done very recently. The double differences in symmetry energies of neighbouring nuclei have the advantage that effects from pairing and shell corrections are well cancelled out, resulting in a compact correlation between the double differences and the mass number of nuclei. This yields values of $C_{\rm v}(\rho_0)$ and $C_{\rm s}$ as 32.1±0.31 MeV and 58.91 ±1.08 MeV, respectively. The uncertainties in $C_{\rm v}(\rho_0)$ and $C_{\rm s}$ are much smaller than those found previously.

For a finite nucleus of mass number A, the symmetry coefficient $a_{\rm sym}(A)$ is always less than $C_{\rm v}(\rho_0)$. The coefficient $a_{\rm sym}(A)$ can be equated to $C_{\rm v}(\rho_A)$ [5], where ρ_A is an equivalent density, always less than ρ_0. Thus, by using eq. (2),

$$C_{\rm v}(\rho_A) = C_{\rm v}(\rho_0) - C_{\rm s}A^{-1/3}. \tag{3}$$

The left-hand side of the above equation can be expanded around the density ρ_0 as

$$C_{\rm v}(\rho_A) = C_{\rm v}(\rho_0) - L\epsilon_A + \frac{K_{\rm sym}}{2}\epsilon_A^2, \tag{4}$$

where

$$K_{\rm sym} = 9\rho^2\frac{{\rm d}^2C_{\rm v}(\rho)}{{\rm d}\rho^2}\bigg|_{\rho_0} \quad \text{and} \quad \epsilon_A = (\rho_0 - \rho_A)/3\rho_0. \tag{5}$$

Combining eqs (3) and (4) we get

$$C_{\rm s} = A^{1/3}\left[L\epsilon_A - \frac{K_{\rm sym}}{2}\epsilon_A^2\right]. \tag{6}$$

The value of symmetry coefficient $a_{\rm sym}(A)$ or equivalently $C_{\rm v}(\rho_A)$ can also be calculated in the local density approximation as [15]

$$C_{\rm v}(\rho_A) = \frac{1}{AX_0^2}\int {\rm d}^3r\rho(r)C_{\rm v}(\rho(r))[X(r)]^2, \tag{7}$$

where X_0 is the isospin asymmetry (=$(N-Z)/A$) of the nucleus, $\rho(r)$ is the sum of the neutron and proton densities inside the nucleus and $X(r)$ is the local isospin asymmetry.

We start with the ansatz

$$C_{\rm v}(\rho) = C_{\rm v}(\rho_0)\left(\frac{\rho}{\rho_0}\right)^{\gamma}, \tag{8}$$

where γ measures the density dependence of the symmetry energy. In a considerable density range around ρ_0 this ansatz is found to be very consistent with the density dependence obtained from the nuclear equation of state (EOS) with different interactions [1,15,16] and also from experiments in intermediate-energy heavy-ion collisions [2,17]. From eqs (1) and (5) we get,

$$L = 3\gamma C_{\rm v}(\rho_0), \tag{9}$$

and

$$K_{\rm sym} = 9\gamma(\gamma-1)C_{\rm v}(\rho_0). \tag{10}$$

Using eqs (6)–(10), we obtain

$$C_{\rm s} = 3\gamma\epsilon_A C_{\rm v}(\rho_0) A^{1/3}\left[1 - \frac{3}{2}(\gamma - 1)\epsilon_A\right] \tag{11}$$

and

$$(\rho_A)^\gamma = \frac{1}{AX_0^2}\int {\rm d}^3 r\, \rho(r)^{\gamma+1}[X(r)]^2. \tag{12}$$

Given the neutron–proton density profiles in the nucleus, from eq. (12), a chosen value of γ gives ρ_A and hence, ϵ_A. The one that satisfies eq. (11) for given empirical values of $C_{\rm v}(\rho_0)$, $C_{\rm s}$ and ρ_0 is the desired solution for γ. Once γ is known, the equivalent density ρ_A, the symmetry energy slope parameter and symmetry incompressibility are determined. The neutron and proton density profiles are obtained within RMF models. These models are so chosen that they yield the experimental proton rms radius but, neutron rms radius or neutron skin thickness in ^{208}Pb nucleus vary over a wide range. The parameters of the interactions BSR8-BSR14 [18], FSUGOLD [19], NL3 [20] and TM1 [21] have been used to generate the proton and neutron density profiles of ^{208}Pb in the RMF model. In figure 1 we display the values of $C_{\rm v}(\rho_0)$, $L(\rho_0)$ and $r_{\rm skin}$ for the ^{208}Pb nucleus obtained for these different parametrizations of the RMF model.

Ansatz for $C_{\rm v}(\rho)$, different from that given by eq. (8) but consistent with the density dependence obtained from the nuclear EOS with different interactions can also be chosen. As long as the functional form for $C_{\rm v}(\rho)$ depends only on a single parameter, expressions

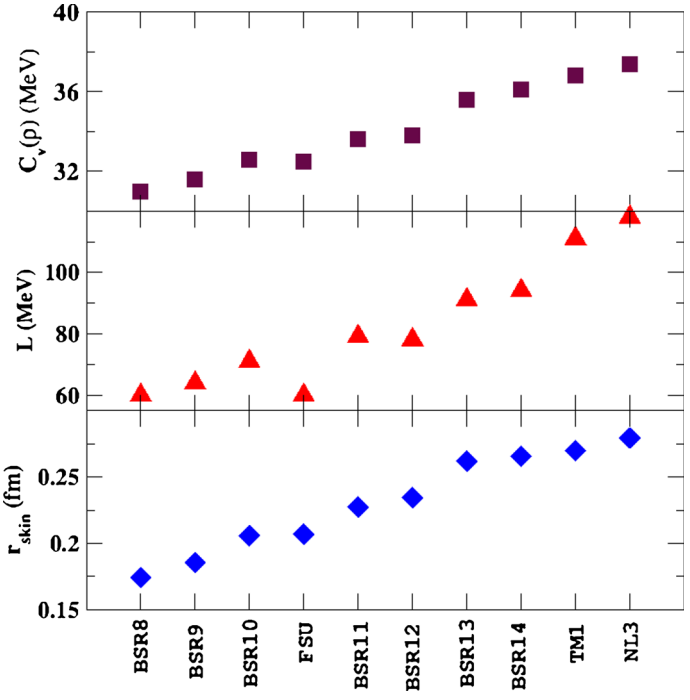

Figure 1. The values of volume symmetry energy coefficient $C_{\rm v}(\rho_0)$, slope parameter $L(\rho_0)$ and neutron skin thickness for ^{208}Pb nucleus for selected RMF models.

analogous to eqs (11) and (12) can be obtained. We have considered a couple of different functional forms for $C_{\rm v}(\rho)$ in addition to that of eq. (8) in order to check the robustness of our results. We use

$$C_{\rm v}(\rho) = C_k\left(\frac{\rho}{\rho_0}\right)^{2/3} + (C_{\rm v}(\rho_0) - C_k)\left(\frac{\rho}{\rho_0}\right)^{\gamma} \tag{13}$$

and

$$C_{\rm v}(\rho) = C_k\left(\frac{\rho}{\rho_0}\right)^{2/3} + C_1\left(\frac{\rho}{\rho_0}\right) + C_2\left(\frac{\rho}{\rho_0}\right)^{5/3}, \tag{14}$$

where

$$C_k = (2^{2/3} - 1)\frac{5}{3}\frac{P_{\rm F,0}^2}{2m^*} \tag{15}$$

is the kinetic energy contribution to the symmetry energy coefficient and

$$C_2 = C_{\rm v}(\rho_0) - C_1 - C_k \tag{16}$$

with $P_{\rm F,0}$ being the Fermi momentum corresponding to the saturation density ρ_0 and m^* is the nucleon effective mass. The functional forms for $C_{\rm v}(\rho)$ given by eqs (13) and (14) have been employed recently in [22] to validate the relationship between $C_{\rm v}$, L and $K_{\rm sym}$

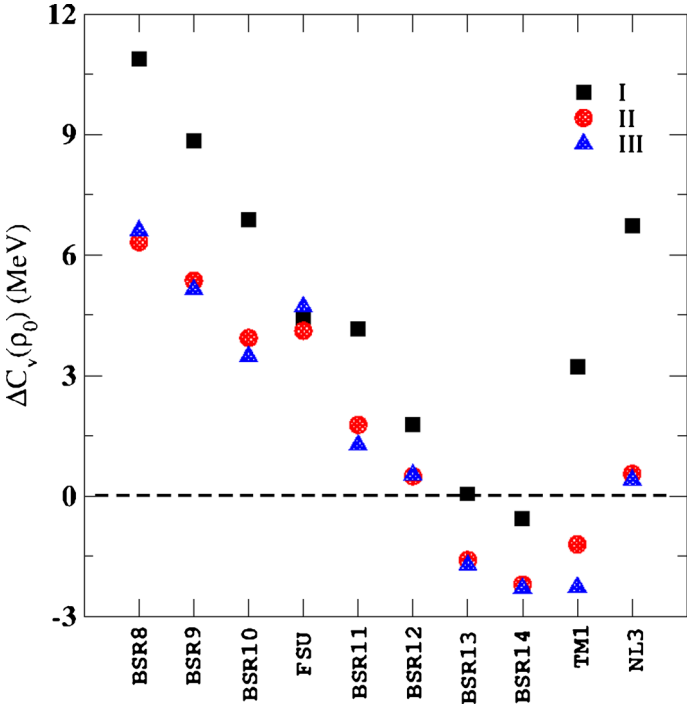

Figure 2. The error $\Delta C_{\rm v}(\rho_0)$ calculated at ρ_0 are shown for various interactions pertaining to Cases I, II and III.

at ρ_0. Hereafter, the different functional forms for $C_v(\rho)$, given by eqs (8), (13) and (14), will be referred to as Case I, II and III, respectively. These cases yield the relations between $C_v(\rho_0)$, L and K_{sym} at density ρ_0 which are as follows:

$$C_v(\rho_0) = \frac{L}{3 + K_{sym}/L}, \tag{17}$$

$$C_v(\rho_0) = C_k + \frac{(L - 2C_k)^2}{3L + K_{sym} - 4C_k} \tag{18}$$

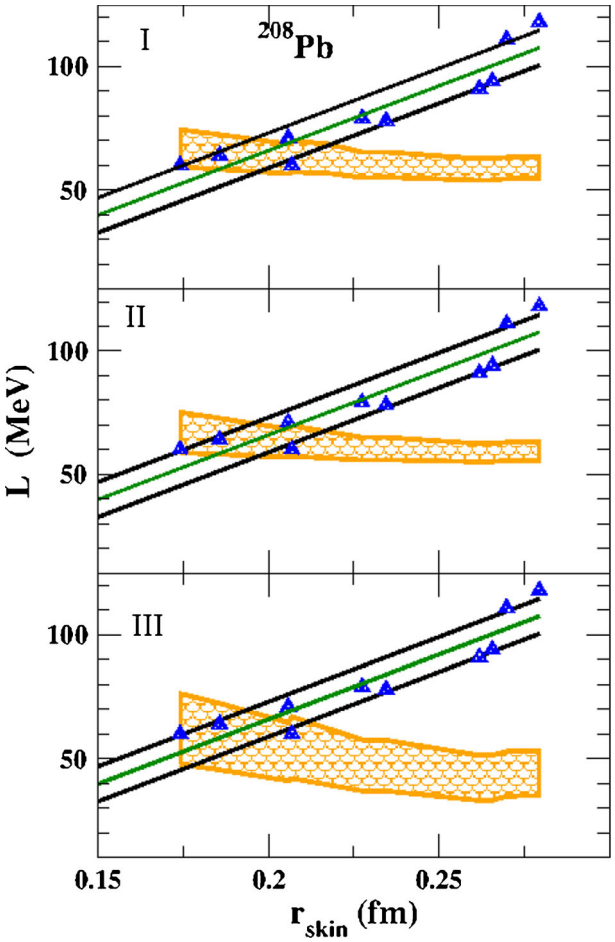

Figure 3. Symmetry slope parameter L plotted as a function of r_{skin} for ^{208}Pb for Cases I, II and III. The blue triangles represent the results for different RMF interactions with L calculated using eq. (1). The green lines with envelopes of slanted black lines refer to the least-squared fits to them with the spread-out error. The shaded regions represent the envelope of possible L values calculated in Cases I, II and III. The intersection of the slanted envelopes and the shaded regions depict the acceptable window for the values of L and r_{skin}.

and

$$C_{\rm v}(\rho_0) = \frac{L}{3} - \frac{K_{\rm sym}}{15} + \frac{C_k}{5}. \tag{19}$$

The results for the error $\Delta C_{\rm v}(\rho_0)$, obtained using different RMF models, are displayed in figure 2. $\Delta C_{\rm v}(\rho_0)$ is the difference between the exact value of $C_{\rm v}(\rho_0)$ and the one calculated using the right-hand side of eqs (17)–(19). The departure of $\Delta C_{\rm v}(\rho_0)$ from zero is indicative of the inaccuracy involved in expressing the functional dependence of symmetry energy. The values of $\Delta C_{\rm v}(\rho_0)$ for Cases II (red circles) and III (blue triangles) are quite similar to the interactions we have chosen; they lie closer to zero in comparison to those in Case I, except for the BSR13 and BSR14 interactions.

In figure 3, we display variations of the symmetry energy slope parameter L as a function of $r_{\rm skin}$ for ^{208}Pb for Cases I, II and III. The values of $r_{\rm skin}$ are calculated using density profiles for protons and neutrons obtained for various RMF interactions. The values of L for the blue triangles are obtained using eq. (1). As usual, almost linear correlations between L and $r_{\rm skin}$ exists. The green straight lines passing through the triangles are obtained by a least-squares fit. The thick black lines are drawn by taking into account the rms error in L due to deviations from the linear correlations between L and $r_{\rm skin}$. We also calculate L using different functional forms for $C_{\rm v}(\rho_0)$ as given by eqs (8), (13) and (14) referred to as Cases I, II and III. The orange-shaded region is obtained by using the empirical values for $C_{\rm v}(\rho_0)$ (=32.1±0.31 MeV), $C_{\rm s}$ (=58.91 ±1.08 MeV) and ρ_0 (=0.155 ±0.008 fm^{-3}). These values display an altogether different type of correlation of L with $r_{\rm skin}$, the weak dependence coming from the imposed empirical constraints. This different behaviour of L with $r_{\rm skin}$, shown by orange-shaded region, stems from the fact that the values of L are calculated by keeping $C_{\rm v}(\rho_0)$ and $C_{\rm s}$ fixed. However, bulk properties of the finite nuclei yield strong correlations of L with $C_{\rm v}(\rho_0)$ and $C_{\rm s}$. The overlap of thick black lines with the orange-shaded region projects out simultaneously, the acceptable values of neutron skin thickness and the density slope parameter L. By combining the results for Cases I, II and III, we get acceptable values of $L = 59 \pm 13$ MeV and $r_{\rm skin} = 0.196 \pm 0.021$ fm for ^{208}Pb nucleus.

3. Conclusions

To conclude, we propose a method to make a simultaneous precision determination of the density slope parameter L for the symmetry energy and the neutron skin thickness of a heavy nucleus by using of the empirical values of volume and surface symmetry energy coefficients extracted from precisely known nuclear masses. As an illustration, we apply our method to the nucleus ^{208}Pb, often taken as a benchmark system to extract the bulk nuclear properties. We obtain $L = 59 \pm 13$ MeV, the neutron skin thickness of ^{208}Pb nucleus comes out to be 0.196 ± 0.021 fm. The nuclear EOS around the saturation density is thus more securely determined; furthermore, the narrow limits on the neutron skin thickness allows for a better feel on the realistic input in the isovector channel in the construction of effective nucleon–nucleon interactions.

References

[1] B-A Li, L-W Chen and C M Ko, *Phys. Rep.* **464**, 113 (2008)
[2] M A Famiano *et al*, *Phys. Rev. Lett.* **97**, 052701 (2006)
[3] J Piekarewicz, B K Agrawal, G Colo, W Nazarewicz, N Paar, P-G Reinhard, X Roca-Maza and D Vretenar, *Phys. Rev. C* **85**, 041302 (2012)
[4] A W Steiner and Gandolfi, *Phys. Rev. Lett.* **108**, 081102 (2012)
[5] M Centelles, X Roca-Maza, X Vias and M Warda, *Phys. Rev. Lett.* **102**, 122502 (2009)
[6] P-G Reinhard and W Nazarewicz, *Phys. Rev. C* **81**, 051303 (2010)
[7] C J Horowitz, S J Pollock, P A Souder and R Michaels, *Phys. Rev. C* **63**, 025501 (2001)
[8] S Abrahamyan *et al*, *Phys. Rev. Lett.* **108**, 112502 (2012)
[9] J D Donnelly and I Sick, *Nucl. Phys. A* **503**, 589 (1989)
[10] J Piekarewicz, *Phys. Rev. C* **83**, 034319 (2011)
[11] A Tamii *et al*, *Phys. Rev. Lett.* **107**, 062502 (2011)
[12] B K Agrawal, J N De and S K Samaddar, *Phys. Rev. Lett.* **109**, 262501 (2012)
[13] B K Agrawal, J N De, S K Samaddar, G Colo and A Sulaksono, *Phys. Rev. C* **87**, 051306(R) (2013)
[14] H Jiang, G J Fu, Y M Zhao and A Arima, *Phys. Rev. C* **85**, 024301 (2012)
[15] S K Samaddar, J N De, X Vinas and M Centelles, *Phys. Rev. C* **76**, 041602(R) (2007)
[16] L-W Chen, C M Ko and B-A Li, *Phys. Rev. Lett.* **94**, 032701 (2005)
[17] D V Shetty, S J Yennello and G A Souliotis, *Phys. Rev. C* **76**, 024606 (2007)
[18] S K Dhiman, R Kumar and B K Agrawal, *Phys. Rev. C* **76**, 045801 (2007)
[19] B G Todd-Rutel and J Piekarewicz, *Phys. Rev. Lett.* **95**, 122501 (2005)
[20] G A Lalazissis, J Konig and P Ring, *Phys. Rev. C* **55**, 540 (1997)
[21] Y Sugahara and H Toki, *Nucl. Phys. A* **579**, 557 (1994)
[22] J Dong, W Zuo, J Gu and U Lombardo, *Phys. Rev. C* **85**, 034308 (2012)